Research Article | Vol. 28, No. 16 / 3 August 2020 / Optics Express 23133
Optics EXPRESS

Resonant opto-mechanical modulators and switches by femtosecond laser micromachining

MICHELE SPAGNOLO,[1,3] RICCARDO MOTTA,[1,3] ROBERTO MEMEO,[1,2] FRANCESCO PELLEGATTA,[1,2] ANDREA CRESPI,[1,2,*] AND ROBERTO OSELLAME[1,2]

[1]Dipartimento di Fisica - Politecnico di Milano, p.za Leonardo da Vinci 32, 20133 Milano, Italy
[2]Istituto di Fotonica e Nanotecnologie - Consiglio Nazionale delle Ricerche (IFN-CNR), p.za Leonardo da Vinci 32, 20133 Milano, Italy
[3]These authors equally contributed to this work
[*]andrea.crespi@polimi.it

Abstract: In this work we demonstrate novel integrated-optics modulators and switches, realized in a glass substrate by femtosecond laser pulses. These devices are based on oscillating microcantilevers, machined by water-assisted laser ablation. Single-mode optical waveguides are laser-inscribed inside the cantilever beam and continue in the substrate beyond the cantilever's tip. By exciting the resonant oscillation of the mechanical structure, coupling between the waveguide segments is varied in time. Operation frequencies are in the range of tens of kilohertz, thus they markedly overcome the response-time limitation of other glass-based modulators, which rely on the thermo-optic effect. These components may be integrated in more complex waveguide circuits or optofluidic lab-on-chips, to provide periodic and high-frequency modulation of the optical signals.

1. Introduction

Fiber-optic networks and integrated waveguide circuits, dedicated to the most diverse applications, make fundamental use of optical modulators and switches, i.e. components that can dynamically vary the intensity of the optical signal or route it into different paths.

Telecommunication applications may require operation frequencies in the megahertz or even gigahertz range. Such high modulation frequencies can be reached by exploiting the electro-optic effect in nonlinear substrates such as lithium niobate [1], or carrier injection in semiconductors such as silicon [2].

A flourishing field of application of integrated-optic technologies is optical sensing and biochemical analysis on lab-on-chip optofluidic devices [3–5]. In these contexts, requirements on the modulation frequency may be less stringent than in telecommunications. In addition, the use of nonlinear substrates or semiconductors is not compatible with many applications, in particular in the biophotonics field, due to their high cost, limited transparency, and possible high chemical reactivity and toxicity.

Glass materials typically present wide transparency windows, from the near infrared up to the whole visible region, have low chemical reactivity and excellent bio-compatibility. Although silica waveguides can be fabricated by conventional photolithography on silicon substrates [6], high-quality waveguides can also be directly inscribed in the bulk of several different glass substrates by means of femtosecond laser micromachining [7–9]. The latter technology enables the realization of advanced devices, which combine refractive index modifications with complex microstructuring of the material [10,11].

Realizing fast optical modulators in glass is not an easy task, because of the lack of nonlinearity and conductive properties. Thermo-optic phase modulators, which exploit refractive index variations induced by local heating, are widely employed to reconfigure silica-on-silicon

#396513 https://doi.org/10.1364/OE.396513
Journal © 2020 Received 30 Apr 2020; revised 5 Jun 2020; accepted 16 Jun 2020; published 20 Jul 2020

Optics EXPRESS

integrated circuits [6]. More recently, such thermal phase shifters have been demonstrated also in femtosecond-laser written devices [12]. While a notable level of complexity can be reached [13–15], the main drawback of this approach resides in the slow response time, which is determined by the dynamics of the thermal diffusion in the substrate and is typically limited to the millisecond range [16].

In this work we propose and demonstrate a new concept for intensity modulators and switches in integrated optics, which operate periodically at the frequency of tens of kilohertz. These devices are based on the resonant oscillation of a microcantilever, which contains a waveguide embedded in the beam. One or more waveguides continue in the bulk substrate after the cantilever's tip and can be periodically coupled and uncoupled to the waveguide in the cantilever, during the oscillations of the latter. Fabrication is entirely performed by means of femtosecond laser pulses, by combining water-assisted laser ablation of the mechanical microstructures and laser waveguide writing.

2. Methods

The opto-mechanical devices are machined by femtosecond laser pulses in a commercial alumino-borosilicate glass (Eagle XG, Corning). In detail, a fiber-based Ytterbium laser is employed (Amplitude Satsuma), which delivers 250-fs pulses with energy up to 10 μJ. The irradiation pattern in the glass substrate is traced by moving the glass sample with respect to the laser focus, using high-accuracy 3-axis translation stages (Aerotech ANT130).

The inscription of the optical waveguides and the mechanical microstructuring are both performed, for each device, in the same fabrication session. This guarantees a relative alignment within the precision of the translation stages, which is better than 100 nm. The glass sample, immersed in water, is machined with laser pulses that are focused by a 20× water-immersion objective (Zeiss N-Achroplan). Immersion in a liquid environment enhances the efficacy of the ablation process and mitigates spherical-aberration effects at the glass interfaces, providing more uniform focusing conditions along the entire sample thickness.

Microstructuring of the cantilevers is performed by water-assisted laser ablation, proceeding upwards from the bottom surface. The cavities to be ablated are divided into box-shaped regions. Only the external surfaces of each box are processed, so that after irradiation the internal glass block drops out; glass excavation proceeds by sequential removal of small blocks in convenient order. Irradiation parameters for ablation are 50 kHz pulse repetition rate, 1.8 μJ pulse energy and translation speed of 2 mm s^{-1}; adjacent irradiation tracks are separated by 1.0 μm.

Waveguides are inscribed by a single laser scan, using 1 MHz repetition rate, 350 nJ pulse energy and translation speed of 10 mm s^{-1}. Such irradiation parameters produce single-mode waveguides at 1.55 μm wavelength, with mode size of about 13 μm ($1/e^2$ diameter). Coupling loss with standard single-mode fiber are estimated to be about 0.5 dB and propagation losses < 0.8 dB cm^{-1}.

The laser-machining time for one complete device does not exceed 30 minutes, where most of the time is employed by the ablation process.

Finally, an ultrasound bath is used to facilitate debris removal from the ablated cavities. Input and output facets of the glass samples are ground and polished at optical quality. A preliminary characterization is performed on all the fabricated devices. An optical fiber is then permanently fixed (by UV-curing glue) at the input port of selected devices, to ensure stable coupling during the mechanical operation.

In our characterization experiments, the oscillation of the cantilever is obtained by forcing an oscillation of the whole glass chip, using a piezoelectric disc actuator (Physik Instrumente). In detail, the driving voltage is provided by an electronic function generator, whose output signal is amplified by a factor of ~3 and impedance-adapted to the piezo, using a custom-assembled electrical transformer. Light from a 1550 nm wavelength laser diode is injected in the input port

Optics EXPRESS

by means of the glued fiber. The optical power at the output is collected by an objective and sent to a power-meter head or to a fast photodiode.

3. Operation principles

Our opto-mechanical devices are based on cantilever structures, containing an optical waveguide. One or more waveguides are continuing in the substrate, beyond the cantilever's tip. To operate the device, a mechanical oscillation of the cantilever is excited at its fundamental resonance frequency. During the oscillation, the output port of the embedded waveguide (placed on the cantilever's tip) is periodically coupled to the input ports of the other waveguide segments continuing in the substrate.

A first kind of device (Fig. 1(a)) is provided with only one waveguide segment continuing in the substrate, aligned with the rest position of the cantilever. In this case a peak of maximum transmission is obtained when the cantilever passes through its rest position, while lateral displacement of the cantilever's tip produces a modulation of the transmitted power. Since the cantilever passes through its rest position twice per oscillation cycle, the modulation occurs at a frequency which is twice the frequency of the mechanical oscillation.

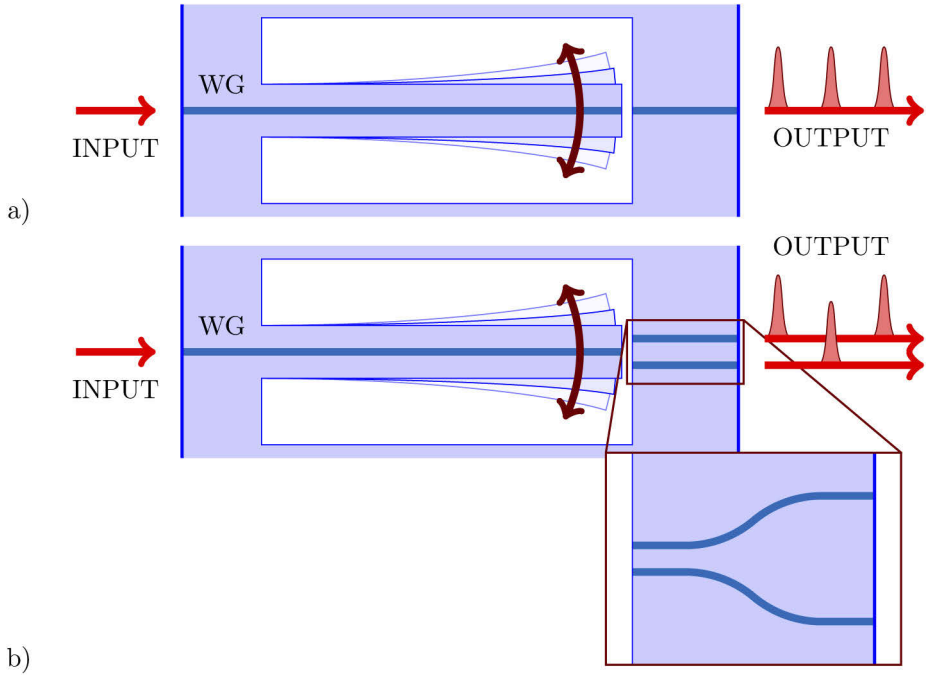

Fig. 1. (a) Concept scheme of the intensity modulator based on a cantilever with one optical waveguide inscribed in it, and one waveguide continuing in the substrate after the cantilever's tip. Coupling between the two waveguide segments is modulated by the cantilever oscillations. (b) Concept scheme of the switch: it is similar to the modulator but here two waveguides find place after the cantilever. They are alternately coupled during the oscillations. As shown in the inset, the two waveguides actually start at a close relative distance, to enable the device operation with relatively small oscillation amplitude, and then separate at larger distance to be addressed more conveniently at the output of the chip.

A second kind of device (Fig. 1(b)) presents two waveguides departing in the bulk substrate, separated by several microns and placed symmetrically with respect to the center of oscillation. When the oscillation of the cantilever is driven with adequate amplitude, the output at the

Optics EXPRESS

cantilever's tip is alternately coupled to such two waveguides. Thus, the device operates as a periodic switch.

The natural oscillation modes of our mechanical structures can be predicted analytically, with good approximation, using the Euler-Bernoulli beam theory. In detail, the resonance frequencies of a cantilevered beam with rectangular cross-section are given by [17]:

$$F_n = R_n^2 \frac{\pi t}{4L^2} \sqrt{\frac{E}{3\rho}} \tag{1}$$

where L is the length of the cantilever, t is the thickness (parallel to the direction of oscillation), ρ is the material density and E is the Young modulus (see also the dimensional scheme in Fig. 2(a)). One notes that the cantilever's height b does not influence F_n. The coefficients R_n, which are also a function of the mode order n, take the values $R_1 \simeq 0.597$ and $R_2 \simeq 1.494$ for the first and second order mode respectively. Relevant mechanical properties for Eagle XG glass are $\rho = 2380$ kg m^{-3} and $E = 73.6$ GPa.

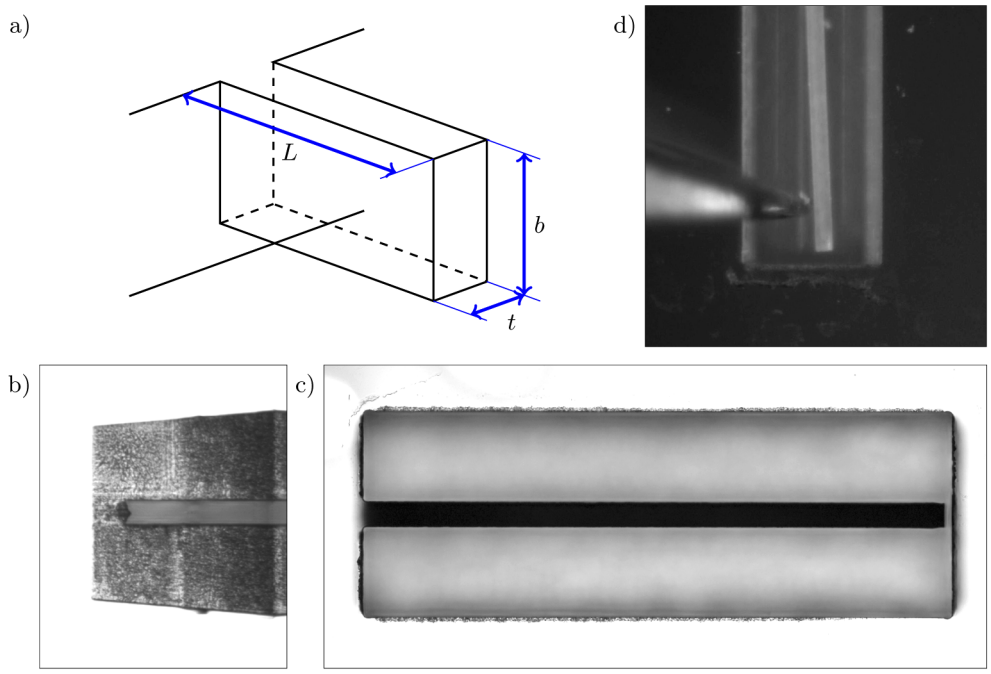

Fig. 2. (a) Dimensional schematic of the cantilever structure. (b)-(c) Microscope pictures of one of the fabricated devices, as observed from the side and from the top surface of the chip. For this structure $L \simeq 1.0$ mm. (d) A cantilever is slightly deflected by gently pushing its tip with a needle.

If oscillation amplitudes are not too large and the system is kept within the linear regime, the periodic deformation of the piezo-actuator is transferred to the displacement of the cantilever's tip (with respect to its rest position) by the complex transfer function:

$$T(f) = \frac{f\left(f - j\frac{F_n}{Q}\right)}{(F_n^2 - f^2) + j\frac{F_n}{Q}f} \tag{2}$$

where F_n is the resonance frequency and Q is the quality factor. At resonance, i.e. for $f \sim F_n$, the modulus of (2) tends to coincide with Q. For cantilevers comparable to ours in size, and

Optics EXPRESS

immersed in air at ambient pressure, damping is mainly due to air friction [18] and that is the main limiting factor for Q.

4. Experimental results

4.1. Optical intensity modulator

We fabricated several devices with the layout in Fig. 1(a). In detail, the cantilevers were designed with nominal dimensions t = 50 μm, b = 250 μm and L spanning from 1.0 mm to 1.5 mm, to implement different resonance frequencies. The large difference between t and b allows to separate in frequency the modes of oscillation in the plane of the substrate from those off-plane.

Due to fabrication tolerances, the dimensions of the realized structures were slightly different from the nominal ones. In particular, upon measurement with an optical microscope, the thickness and height resulted to be respectively $t \simeq 40$ μm and $b \simeq 240$ μm. The gap between the tip and the rest of the substrate was typically around 15 μm. Figure 2(b)-(d) reports microscope pictures of one of the fabricated devices.

Optical insertion loss of the entire device (about 2 cm long) is about 8 dB, when the cantilever is perfectly aligned. Given the characterized values of coupling and propagation loss for the inscribed waveguides, we mainly attribute the insertion loss of the device to the air gap between the cantilever's tip and the rest of the substrate. In particular, we believe that the rough interfaces, resulting from laser ablation, are the major cause for this loss. Additional work is needed to improve the quality of the ablated surfaces; to this purpose laser-ablation parameters may be optimized on an extended range, and thermal-annealing processes (following fabrication) [19] could be investigated.

After connecting an optical fiber to the input port, the resonance frequencies of the cantilever structures were experimentally retrieved. The frequency of the sinusoidal driving voltage was swept from a few kHz to 1 MHz frequency, while keeping the amplitude constant (20 V peak-to-peak on the piezo-actuator contacts). Frequencies that provided a non-negligible modulation of the output optical signal are reported in Table 1. It was possible to clearly identify the first and second in-plane oscillation modes of each of the fabricated devices: their experimentally-measured frequencies show excellent agreement with the theoretical predictions obtained from Eq. (1).

Table 1. Experimental (f_{exp}) and theoretical (f_{theo}) resonance frequencies for first and second order modes of in-plane oscillation of the fabricated cantilever structures. The experimental values are measured as explained in the main text. The theoretical values are calculated by substituting in Eq. (1) the actual dimensions of the fabricated structures, L_{exp} and t_{exp}, as measured using an optical microscope.

	L_{exp} = 1.0 mm		L_{exp} = 1.2 mm		L_{exp} = 1.5 mm	
	t_{exp} = 40 μm		t_{exp} = 38 μm		t_{exp} = 41 μm	
Mode order	f_{exp}	f_{theo}	f_{exp}	f_{theo}	f_{exp}	f_{theo}
1	36.0 kHz	35.9 kHz	23.8 kHz	23.7 kHz	16.1 kHz	16.4 kHz
2	223 kHz	225 kHz	149 kHz	149 kHz	101 kHz	103 kHz

The device operation was characterized as a function of the amplitude of the driving signal (from 0 V to 86 V peak-to-peak, measured after the transformer), keeping the frequency fixed in correspondence to the first oscillation mode. As a significant figure of merit, we define the Extinction Ratio (E.R.) as:

$$\text{E.R.}|_{\text{dB}} = 10 \log_{10} \frac{P_{max}}{P_{min}} \tag{3}$$

Optics EXPRESS

where P_{min} and P_{max} are the minimum and maximum transmitted optical power in an oscillation cycle, as read by the photodiode.

Figure 3(a) reports the measured E.R. as a function of the peak-to-peak signal amplitude on the piezo-actuator, for the cantilever with $L = 1.0$ mm. The E.R can reach and exceed 19 dB for a 86-V peak-to-peak driving sinusoid. Figure 3(b) plots the acquired output signal when the highest driving voltage was used: the light is modulated in a train of pulses at about 72 kHz, i.e. twice the driving frequency.

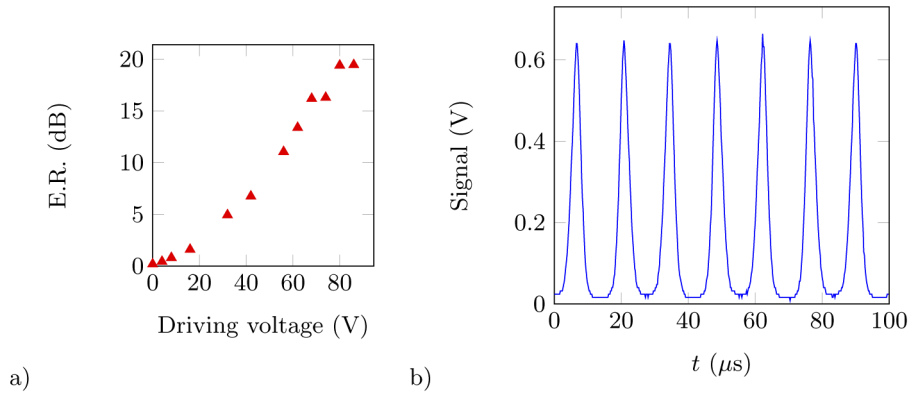

Fig. 3. Characterization of the intensity modulator, based on a cantilever with $L = 1.0$ mm. (a) Measured E.R. for different amplitudes of the sinusoidal driving signal of the piezo-actuator (peak-to-peak voltage). (b) Measured signal at the photodetector when a 86-V peak-to-peak sinusoid is applied to the piezo-electric actuator. High-frequency noise was digitally filtered from the signal.

Finally, we performed a more detailed study of the response of the micromechanical systems around the resonance. The frequency of the sinusoidal driving voltage of the piezo-actuator was finely swept around the resonance, while keeping the amplitude fixed at 40 V peak-to-peak. From the amplitude of the optical modulation, detected by the photodiode, it was possible to retrieve the amplitude of mechanical oscillation of the cantilever for each frequency (see Appendix A). Figure 4 reports the retrieved resonance peak, in the case of the cantilever with length $L = 1.0$ mm. By fitting $|T(f)|$ on the experimental curve it was possible to obtain the Q factor of the mechanical oscillator, which is estimated in this case to be about 300.

4.2. Two-port switch

The second device we demonstrate is an optical switch based on the same kind of oscillating cantilever. Facing the cantilever's tip, two waveguides find place, which bring to two distinct output ports of the device (Fig. 1(b)). The cantilever oscillation alternately excites either one of them.

At the output facet of the chip, such two waveguides are at a relative distance of 127 μm, which is a standard for possible connection with fiber arrays. However, at their starting point, they need to be placed at sufficiently small distance, in order to be both reached by the cantilever oscillation without increasing excessively the oscillation amplitude. At the same time, their separation must be larger than the guided mode size, in order to allow their individual excitation. As a compromise between the above discussed requirements, we chose a starting distance between the output waveguides of 13 μm. The radius of curvature of the bent waveguide segments was 90 mm, which guarantees additional bending losses lower than 0.1 dB.

Evanescent-field coupling, for waveguides that run parallel at 13 μm distance, is small but not negligible. Such coupling can lead to power transfer from one waveguide to the other and may

Optics EXPRESS

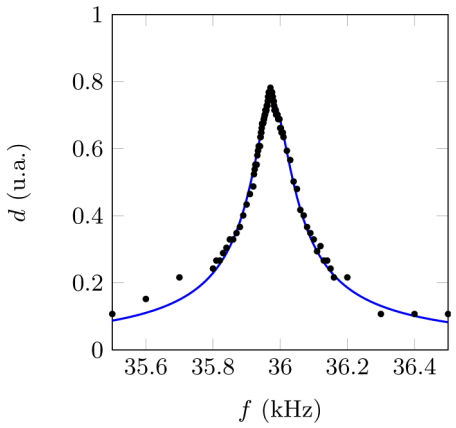

Fig. 4. Amplitude of the cantilever oscillation as a function of the driving frequency. The continuous line is best fit of the experimentally retrieved values (shown as black dots), with a function of the kind of Eq. (2), multiplied by a proper constant.

deteriorate the isolation of one output port with respect to the other one. Instead of distancing the waveguides farther apart, trying to reduce the coupling in absolute terms, we chose to engineer the waveguide path in such a way that evanescent-field coupling fully transfers the optical power from one waveguide to the other. Namely, when the cantilever's tip is facing the upper output waveguide, light is fully transferred to the lower one by evanescent-field interaction and, vice versa, when the cantilever's tip is facing the lower waveguide light is transferred to the upper one. In detail, this is accomplished by making the waveguides to run parallel for 1.88 mm, at 13 μm distance, before separating following the S-bends with 90 mm curvature radius. Such design was optimized prior to the fabrication of the switch, by inscribing and characterizing directional couplers with different geometries on a separate chip.

The resonant optical switch was fabricated with the same method and irradiation parameters used for the intensity modulator. The cantilever dimensions were analogous to the previous ones; in detail t = 50 μm, b = 250 μm and L =1.0 mm.

Characterization and actuation of the mechanical oscillations were also performed as in the previous case. To locate the fundamental oscillation frequency, the modulation on one of the two output signals was monitored while sweeping the excitation frequency of the piezo-actuator. The

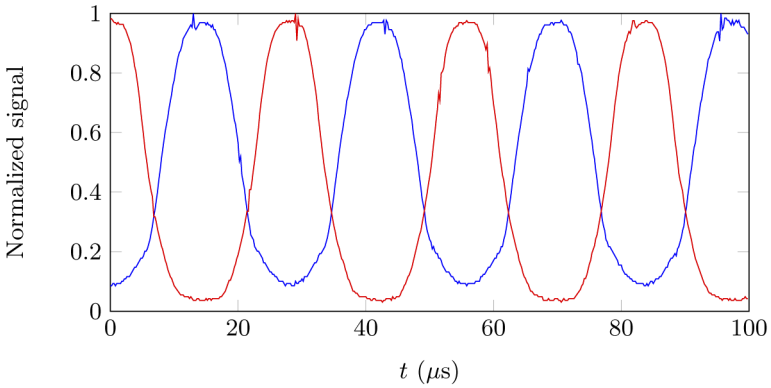

Fig. 5. Output signals of the two-port switch, as a function of time. The signal of each port has been normalized to its maximum value.

Optics EXPRESS

device performance was then assessed by selecting the correct frequency and by increasing the voltage of the actuation signal until optimal modulation conditions are reached.

Figure 5 shows the modulated optical signals from the two output ports of the device, normalized to the respective maximum, as acquired for a sinusoidal actuation voltage of the piezo of 30.6 V peak-to-peak. Contrast ratio between the maximum and minimum signal exceeds 10 dB for both channels. The insertion loss of the device, in correspondence of the peaks of transmission, is 10.4 dB from input to output 1 and 11.7 dB from input to output 2 (red and blue curve, respectively, in Fig. 5). The different transmission of the two channels can be attributed to irregular roughness of the glass-air interfaces.

5. Discussion and conclusions

We have designed and demonstrated micro-mechanical optical modulators and switches, based on oscillating cantilevers excited at one of their natural resonance frequencies. The devices are entirely fabricated by femtosecond laser pulses, combining water-assisted laser ablation and direct waveguide inscription.

In particular, we have shown a modulation of the optical signal on a single channel with E.R. higher than 19 dB at a frequency of ~72 kHz, and switching between two optical channels at a frequency of ~36 kHz. These performances neatly overcome, in terms of frequency, the possibilities of standard integrated modulators in glass, based on the thermo-optic effect.

The operation frequency of the devices can be adjusted by design, by changing the size of the resonating structures, e.g. the cantilever length. We envisage that fine tuning of the oscillation frequency could be achieved even after fabrication, by employing the same femtosecond laser to perform microablations in defined points on the cantilever structure. In particular, material removal from the cantilever's tip should reduce the effective mass of the oscillator and thus increase its oscillation frequency; material removal close to the basis should instead mainly reduce the effective stiffness of the structure, thus producing the opposite effect.

In addition, femtosecond laser writing allows to fabricate single-mode waveguides for different wavelength ranges, from the visible to the near-infrared, in the same glass substrate upon proper optimization of the irradiation parameter [12,15,20]. Thus, while the present devices have been developed for the telecom range, analogous components may be fabricated for different wavelengths. Improved propagation losses and smaller mode size could be obtained by adopting a multi-scan waveguide writing approach [21].

In perspective, these devices could be included in more complex networks of waveguides or fiber components. In particular, they could be integrated in lab-on-a-chip devices, where fluidic microchannels could be machined by the same femtosecond laser technology. Femtosecond laser irradiation followed by chemical etching could be also adopted for defining the mechanical structures [11,22]. Furthermore, oscillating resonant structures similar to the ones reported here, but immersed in liquid, might also be employed as viscosity sensors for the surrounding fluid.

A. Modelling optical transmission

The optical transmission of our devices is determined by the overlap between the optical mode exiting from the waveguide in the cantilever and the optical mode of the waveguide continuing in the substrate. These two modes can be laterally displaced by a distance d, which depends on the amount of deformation of the cantilever. In the case of the intensity modulator, ideally $d = 0$ when the cantilever's tip passes in the center of the oscillation. In the case of the switch, considering one of the two output ports, $d = 0$ when the instantaneous deformation of the cantilever is such that its tip is facing the input of the corresponding waveguide.

Optics EXPRESS

Approximating the two modes as Gaussian, and neglecting radial phase terms, the overlap integral is written as:

$$OI = \frac{2}{\pi w_1 w_2} \iint exp\left(-\frac{x^2+y^2}{w_1^2}\right) \cdot exp\left(-\frac{(x-d)^2+y^2}{w_2^2}\right) dx\, dy \tag{4}$$

where x and y are transverse coordinates and $w_{1,2}$ are the mode radii. The coupling efficiency is $\eta = |OI|^2$ and can be calculated as:

$$\eta = \eta_0 e^{-\frac{d^2}{\sigma^2}} \tag{5}$$

where:

$$\sigma^2 = \frac{w_1^2 + w_2^2}{2} \qquad \eta_0 = \frac{4w_1^2 w_2^2}{\left(w_1^2 + w_2^2\right)^2} \tag{6}$$

Considering more specifically the conditions of our devices, on the side of the receiving waveguide, $w_2 = w_0$ coincides with the size of the guided mode, which is measured to be $w_0 \sim 6.5\ \mu$m (see the Methods section). On the side of the beam exiting the cantilever's tip, in principle, one should take into account some divergence due to free space propagation. However, in our conditions and given $\lambda = 1.55\ \mu$m, the Rayleigh range is in the order of $z_R = \pi w_0^2/\lambda \simeq 86\ \mu$m, which is much wider than the air gap ($\sim$15 μm). Thus, no sensible enlargement of the spot size should be due to this cause and we should have also $w_1 = w_0$. In addition, within the Rayleigh range the phase front is almost flat; this supports the approximation of neglecting radial phase terms.

As a matter of fact, the roughness of the ablated glass walls have diffusive effects on light, i.e. light is partially transferred to higher-order modes of the Hermite-Gauss basis. However, we can still consider Eq. (5) as an approximation which just takes into account the projection on the first order mode, with parameters η_0 and σ that may be slightly different from the ideal ones.

By inverting Eq. (5) it is possible to calculate d, i.e. the amplitude of the cantilever's tip oscillation, from the value of η.

$$d = \sigma\sqrt{\log\frac{\eta_0}{\eta}} \tag{7}$$

The efficiency η can indeed be retrieved from the amplitude of the optical modulation.

We note that σ is just a multiplication factor. To obtain the values plotted in Fig. 4 we left σ undetermined and we expressed d in arbitrary units (a.u.).

Funding

H2020 European Research Council (742745, CAPABLE).

Acknowledgments

The authors would like to thank Dr. Francesco Ceccarelli for useful discussions and for realizing the custom-made electrical transformer employed to drive the piezo-actuator. R.O. acknowledges funding from the European Research Council (ERC) under the European Union's Horizon 2020 research and innovation programme (grant agreement No. 742745, CAPABLE).

Disclosures

The authors declare no conflicts of interest.

Optics EXPRESS

References

1. K. Liu, C. R. Ye, S. Khan, and V. J. Sorger, "Review and perspective on ultrafast wavelength-size electro-optic modulators," Laser Photonics Rev. **9**(2), 172–194 (2015).
2. G. T. Reed, G. Mashanovich, F. Y. Gardes, and D. Thomson, "Silicon optical modulators," Nat. Photonics **4**(8), 518–526 (2010).
3. B. Kuswandi, J. Huskens, N. Nuriman, and W. Verboom, "Optical sensing systems for microfluidic devices: a review," Anal. Chim. Acta **601**(2), 141–155 (2007).
4. C. Li, G. Bai, Y. Zhang, M. Zhang, and A. Jian, "Optofluidics refractometers," Micromachines **9**(3), 136 (2018).
5. N. Wang, T. Dai, and L. Lei, "Optofluidic technology for water quality monitoring," Micromachines **9**(4), 158 (2018).
6. N. Takato, K. Jinguji, M. Yasu, H. Toba, and M. Kawachi, "Silica-based single-mode waveguides on silicon and their application to guided-wave optical interferometers," J. Lightwave Technol. **6**(6), 1003–1010 (1988).
7. G. Della Valle, R. Osellame, and P. Laporta, "Micromachining of photonic devices by femtosecond laser pulses," J. Opt. A: Pure Appl. Opt. **11**(1), 013001 (2009).
8. H. L. Butcher, D. G. MacLachlan, D. Lee, R. R. Thomson, and D. Weidmann, "Demonstration and characterization of ultrafast laser-inscribed mid-infrared waveguides in chalcogenide glass ig2," Opt. Express **26**(8), 10930–10943 (2018).
9. T. T. Fernandez, S. Gross, A. Arriola, K. Privat, and M. J. Withford, "Revisiting ultrafast laser inscribed waveguide formation in commercial alkali-free borosilicate glasses," Opt. Express **28**(7), 10153–10164 (2020).
10. Y. Bellouard, A. A. Said, and P. Bado, "Integrating optics and micro-mechanics in a single substrate: a step toward monolithic integration in fused silica," Opt. Express **13**(17), 6635–6644 (2005).
11. R. Osellame, H. J. Hoekstra, G. Cerullo, and M. Pollnau, "Femtosecond laser microstructuring: an enabling tool for optofluidic lab-on-chips," Laser Photonics Rev. **5**(3), 442–463 (2011).
12. F. Flamini, L. Magrini, A. S. Rab, N. Spagnolo, V. D'Ambrosio, P. Mataloni, F. Sciarrino, T. Zandrini, A. Crespi, R. Ramponi, and R. Osellame, "Thermally reconfigurable quantum photonic circuits at telecom wavelength by femtosecond laser micromachining," Light: Sci. Appl. **4**(11), e354 (2015).
13. J. Carolan, C. Harrold, C. Sparrow, E. Martín-López, N. J. Russell, J. W. Silverstone, P. J. Shadbolt, N. Matsuda, M. Oguma, M. Itoh, G. D. Marshall, M. G. Thompson, J. C. F. Matthews, T. Hashimoto, J. L. O'Brien, and A. Laing, "Universal linear optics," Science **349**(6249), 711–716 (2015).
14. I. Dyakonov, I. Pogorelov, I. Bobrov, A. Kalinkin, S. Straupe, S. Kulik, P. Dyakonov, and S. Evlashin, "Reconfigurable photonics on a glass chip," Phys. Rev. Appl. **10**(4), 044048 (2018).
15. E. Polino, M. Riva, M. Valeri, R. Silvestri, G. Corrielli, A. Crespi, N. Spagnolo, R. Osellame, and F. Sciarrino, "Experimental multiphase estimation on a chip," Optica **6**(3), 288 (2019).
16. F. Ceccarelli, S. Atzeni, A. Prencipe, R. Farinaro, and R. Osellame, "Thermal phase shifters for femtosecond laser written photonic integrated circuits," J. Lightwave Technol. **37**(17), 4275–4281 (2019).
17. C. A. V. Eysden and J. E. Sader, "Resonant frequencies of a rectangular cantilever beam immersed in a fluid," J. Appl. Phys. **100**(11), 114916 (2006).
18. J. W. M. Chon, P. Mulvaney, and J. E. Sader, "Experimental validation of theoretical models for the frequency response of atomic force microscope cantilever beams immersed in fluids," J. Appl. Phys. **87**(8), 3978–3988 (2000).
19. F. He, J. Lin, and Y. Cheng, "Fabrication of hollow optical waveguides in fused silica by three-dimensional femtosecond laser micromachining," Appl. Phys. B **105**(2), 379–384 (2011).
20. G. Douglass, F. Dreisow, S. Gross, and M. Withford, "Femtosecond laser written arrayed waveguide gratings with integrated photonic lanterns," Opt. Express **26**(2), 1497–1505 (2018).
21. A. Arriola, S. Gross, N. Jovanovic, N. Charles, P. G. Tuthill, S. M. Olaizola, A. Fuerbach, and M. J. Withford, "Low bend loss waveguides enable compact, efficient 3d photonic chips," Opt. Express **21**(3), 2978–2986 (2013).
22. A. Crespi, R. Osellame, and F. Bragheri, "Femtosecond-laser-written optofluidics in alumino-borosilicate glass," Opt. Mater. X **4**, 100042 (2019).